Phase diagram of $CuCrO_2$ in a magnetic field

2011 J. Phys.: Condens. Matter 23 366002

(http://iopscience.iop.org/0953-8984/23/36/366002)

J. Phys.: Condens. Matter **23** (2011) 366002 (5pp) doi:10.1088/0953-8984/23/36/366002

Phase diagram of $CuCrO_2$ in a magnetic field

Randy S Fishman

Materials Science and Technology Division, Oak Ridge National Laboratory, Oak Ridge, TN 37831, USA

Received 8 April 2011, in final form 26 July 2011
Published 25 August 2011
Online at stacks.iop.org/JPhysCM/23/366002

Abstract

A simplified model is used to construct the magnetic phase diagram of $CuCrO_2$ as a function of magnetic field and easy-axis anisotropy. Neglecting the weak interactions between hexagonal layers, $CuCrO_2$ is predicted to undergo transitions between three different 3-sublattice (SL) phases with increasing field: from a chiral, non-collinear phase that exhibits multiferroic behavior, to a collinear phase, to a non-chiral, non-collinear phase. The phase diagram also contains 1-SL, 4-SL, and 5-SL collinear phases, some of which may be accessible in the nonstoichiometric compound $CuCrO_{2+\delta}$.

(Some figures in this article are in colour only in the electronic version)

In the recently-discovered 'improper' multiferroic materials [1], the ferroelectric coupling between the magnetization and the electric polarization coincides with the appearance of a non-collinear (NC) magnetic state. Because the ferroelectric coupling allows the electric polarization to be controlled by flipping magnetic domains, it is of great scientific as well as technological interest. Due to the inverse Dzyaloshinskii–Moriya interaction [2], an electric polarization **P** perpendicular to both the spin chirality **C** and the wavevector **Q** has been predicted and observed for improper multiferroics such as $RMnO_3$ (R = Tb or Y), which have spiral spin states with easy-plane anisotropy. However, in at least two classes of improper multiferroics with easy-axis anisotropy, $CuFeO_2$ [3, 4] and $CuCrO_2$ [5, 6], the ferroelectric coupling cannot be explained by the inverse Dzyaloshinskii–Moriya mechanism because **P** is parallel to both **C** and **Q**.

$CuFeO_2$ and $CuCrO_2$ share the same crystal structure with Fe^{3+} or Cr^{3+} ions lying on triangular lattices stacked in an ABC pattern. For both materials, collinear (CL) magnetic order is geometrically frustrated by the antiferromagnetic (AF) interactions $J_1 < 0$ between nearest-neighbor spins within each hexagonal plane. While the nearest-neighbor AF interactions between adjacent hexagonal planes in $CuFeO_2$ are satisfied by most exchange paths with the reversal of the spins in adjacent planes, the interactions between adjacent planes in $CuCrO_2$ are ferromagnetic (FM) and the same spin configuration repeats from one layer to the next. The NC states of both $CuFeO_2$ and $CuCrO_2$ contain spins that lie in the yz plane, perpendicular to both **P** and **C**. It is believed that the ferroelectric coupling in both materials is caused by the modulation of the metal–ligand hybridization with the spin–orbit coupling [7, 8], which implies that **P** is parallel to both **Q** and **C**.

Nevertheless, the multiferroic phases of these two materials differ in important ways. Whereas the NC state of $CuFeO_2$ is incommensurate with wavevector $\mathbf{Q} \approx 0.83\pi\mathbf{x}$ [4] (hexagonal lattice constant set to 1), the NC state of $CuCrO_2$ is almost commensurate with wavevector $\mathbf{Q} \approx (4\pi/3)\mathbf{x}$, corresponding to a unit cell containing 3-sublattices (SLs) [9]. While $CuFeO_2$ becomes multiferroic only with Ga or Al doping [10] or in a magnetic field above 7 T [11, 12], pure $CuCrO_2$ is multiferroic in zero field [5, 6].

For $CuCrO_2$, the small deviation of the ordering wavevector $Q \approx 4\pi/3.04$ from $4\pi/3$ is caused by the weak FM interaction J_z between neighboring planes [13]. Recently, inelastic neutron-scattering measurements of the excitation spectrum of $CuCrO_2$ along the **x** and **z** directions were compared with theoretical predictions based on a Heisenberg model with both easy-plane and easy-axis anisotropies [14]. After adjusting the predicted inelastic intensities to agree with the measured results, this work concluded that $J_z/|J_1| \approx 0.007$ is quite small. Hence a simplified two-dimensional model can be used to construct the magnetic phase diagram of $CuCrO_2$.

As in $CuFeO_2$, the easy-axis anisotropy $-D\sum_i S_{iz}^2$ ($D > 0$) produced by the crystal structure favors CL states aligned along the z axis. Below T_N, magneto-elastic distortions parallel to **Q** [15, 16] modify the exchange parameters

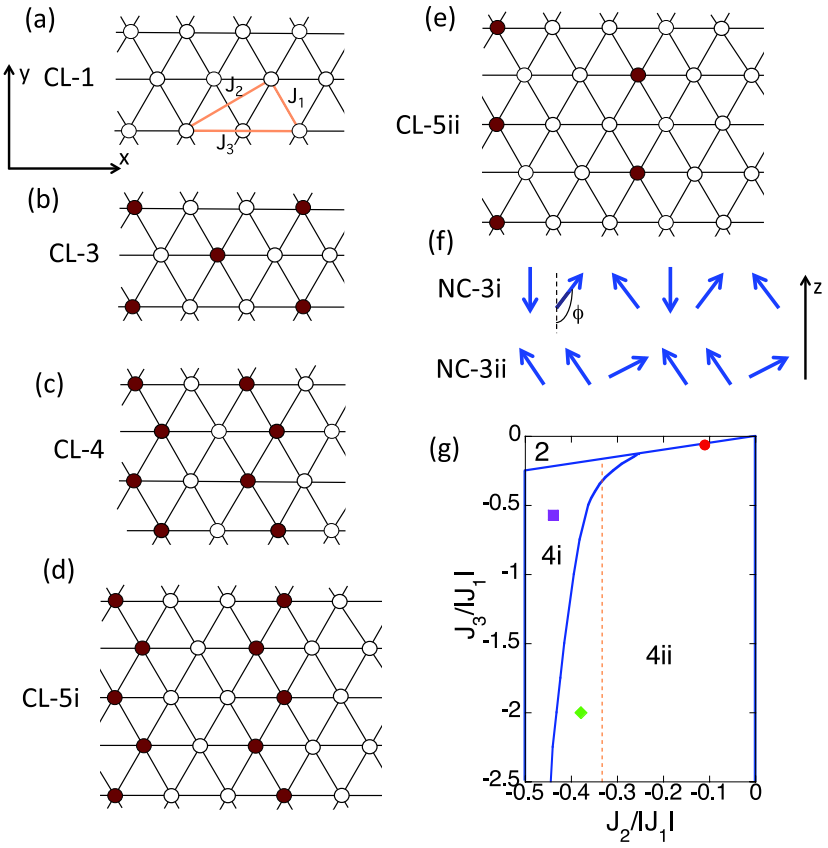

Figure 1. The predicted phase diagram contains: (a) a 1-SL CL phase (also showing the exchange interactions J_n), (b) a 3-SL CL phase, (c) a 4-SL CL phase, (d) a type i 5-SL CL phase that appears to the left of the $J_2/|J_1| = -1/3$ dashed line in (g), and (e) a type ii 5-SL CL phase. White dots indicate up spins and dark dots indicate down spins. (f) Two different 3-SL NC phases with the turn angle ϕ indicated for the NC-3i phase. (g) A portion of the Takagi–Mekata phase space for a triangular-lattice AF at high D and zero field with $J_1 < 0$, showing the 4-SL region with subregions 4i and 4ii and a slice of the 2-SL region at the top. The square, dot, and diamond denote the points $\{J_2/|J_1|, J_3/|J_1|\} = \{-0.44, -0.57\}$, $\{-0.11, -0.06\}$ and $\{-0.38, -2\}$.

within each plane and produce the easy-plane anisotropy $-D_\perp \sum_i S_{ix}^2$ ($D_\perp < 0$). Although the modified exchange interactions remain invariant under a uniform spin rotation, the combination of easy-axis and easy-plane anisotropy breaks that rotational invariance and produces a gap in the spin-wave spectrum. Recent work suggests that the spin-wave gap for $CuCrO_2$ lies between 0.5 and 0.6 meV [13, 14], much larger than the spin-wave gap for the multiferroic phase of Ga-doped $CuFeO_2$ [17]. Fits to the spin-wave spectrum [14] of $CuCrO_2$ indicate that $D/|J_1| \approx 0.17$ and $D_\perp/|J_1| \approx -0.21$.

The energy of $CuCrO_2$ in a magnetic field H along the **z** direction can then be approximated by

$$E = -\tfrac{1}{2}\sum_{i\neq j} J_{ij}\mathbf{S}_i \cdot \mathbf{S}_j - D\sum_i S_{iz}^2 - D_\perp \sum_i S_{ix}^2 - 2\mu_B H \sum_i S_{iz}, \quad (1)$$

where $\mathbf{S}_i \equiv \mathbf{S}(\mathbf{R}_i)$ are classical spins. Exchange pathways for the nearest-neighbor interaction $J_1 < 0$ as well as for the second- and third-neighbor interactions J_2 and J_3 are indicated in figure 1(a). As in $CuFeO_2$ [18], it is likely that excess ($\delta > 0$) or deficient ($\delta < 0$) oxygen acts to increase the easy-axis anisotropy D in the nonstoichiometric compound $CuCrO_{2+\delta}$. Due to the moderate $S = 3/2$ spins in $CuCrO_2$, the assumption of classical spins in equation (1) will incur a somewhat larger error than for the $S = 5/2$ spins of $CuFeO_2$. Nevertheless, equation (1) should provide qualitatively accurate predictions for the phase diagram of $CuCrO_2$ in a magnetic field.

Based on equation (1), the predicted spin states for $CuCrO_2$ are either CL or coplanar. The only effect of the easy-plane anisotropy $D_\perp < 0$ is to rotate the coplanar spins into the yz plane. Since energy differences between the CL or coplanar states are not changed by the easy-plane anisotropy, it will not be explicitly considered in most of the following discussion.

For $D \gg |J_1|$ (Ising spins) and $H = 0$, the phase diagram of equation (1) was constructed by Takagi and Mekata [19]. It contains CL states with 1, 2, 3, 4, or 8 SLs that occupy different portions of $\{J_2/|J_1|, J_3/|J_1|\}$ phase space. The CL-4 region of the $\{J_2/|J_1|, J_3/|J_1|\}$ phase diagram is given by the conditions $J_3 < J_2/2$ and $-0.5 < J_2/|J_1| < 0$.

With the exception of the CL-1 or FM state, all other CL states in the Takagi–Mekata phase diagram become unstable to NC states below critical values of D [20]. As shown in figure 1(g), the 4-SL region contains two subregions: subregion 4ii where the wavevector $\mathbf{Q} = (4\pi/3)\mathbf{x}$

Table 1. Energies and Net Spins of CL states.

Phase	E/NS^2	M_z
CL-1	$-3(J_1+J_2+J_3)-D-h$	1
CL-3	$J_1-3J_2+J_3-D-h/3$	1/3
CL-4	$J_1-J_2+J_3-D$	0
CL-5i	$(J_1+J_2)/5+J_3-D-h/5$	1/5
CL-5ii	$-3(J_1+J_3)/5-7J_2/5-D-3h/5$	3/5

of the NC state at low D is independent of the exchange interactions and subregion 4i where the incommensurate wavevector $\mathbf{Q}$ of the NC state at low D sensitively depends on $\{J_2/|J_1|, J_3/|J_1|\}$ [20][1]. Once in a state with commensurate wavevector $\mathbf{Q} = (4\pi/3)\mathbf{x}$ (region 4ii) or incommensurate wavevector $\mathbf{Q}$ (region 4i), the spin configuration remains commensurate or incommensurate with decreasing D. Hence, the phase boundary between subregions 4i and 4ii in figure 1(g) is independent of D.

Since the wavevector $\mathbf{Q} \approx 0.83\pi\mathbf{x}$ of the NC state for $CuFeO_2$ is incommensurate [4], its exchange parameters must lie within subregion 4i and have been estimated as $\{J_2/|J_1|, J_3/|J_1|\} = \{-0.44, -0.57\}$ [22], indicated by the square in figure 1(g). With wavevector $\mathbf{Q} \approx (4\pi/3)\mathbf{x}$ [9], the exchange parameters of $CuCrO_2$ must lie within subregion 4ii. A recent inelastic neutron-scattering study [13] of $CuCrO_2$ estimated that $J_2/|J_1| = -0.11$. Assuming the small value $J_3/|J_1| = -0.06$, the exchange parameters $\{-0.11, -0.06\}$ of $CuCrO_2$ would be given by the dot just inside region 4ii in figure 1(g). We shall also discuss results for $\{-0.38, -2\}$, given by the diamond on the other side of the dashed vertical line $J_2/|J_1| = -1/3$.

Five different CL states appear in the possible phase diagrams of $CuCrO_2$. The FM or CL-1 state has $M_z = 1$. The CL-3 state has $M_z = 1/3$ and the CL-4 or $\uparrow\uparrow\downarrow\downarrow$ state found in pure $CuFeO_2$ in zero field [3] has $M_z = 0$. Two different 5-SL states appear: the CL-5i or $\uparrow\uparrow\uparrow\downarrow\downarrow$ state with $M_z = 1/5$ and the CL-5ii or $\uparrow\uparrow\uparrow\uparrow\downarrow$ state with $M_z = 3/5$. The energies and net normalized spins of the CL states are summarized in table 1, which defines $h = 2\mu_B H/S$.

As a function of field and anisotropy, trial NC spin states were used to minimize the energy of equation (1). A trial incommensurate state may be [23] built from harmonics of a fundamental ordering wavevector $Q\mathbf{x}$. However, no incommensurate solutions were found in subregion 4ii of the Takagi–Mekata phase diagram. A variational approach with m independent angles θ_n was used to parameterize a commensurate m-SL state with $m \leq 7$.

A general 3-SL NC trial state was constructed using $\mathbf{S}_n = (0, \sin\theta_n, \cos\theta_n)$ with $n = 1$, 2, or 3. At low fields, we obtain the NC-3i state shown in the top of figure 1(f) with $\theta_1 = \pi$ and $\theta_2 = 2\pi - \theta_3 = \pi - \phi$. At higher fields, we obtain the NC-3ii state shown in the bottom of figure 1(f) with $\theta_1 = \theta_2 \neq \theta_3$. Intriguingly, this state exhibits a spontaneous spin $M_y = \langle S_y\rangle/S$ in the $\mathbf{y}$ direction, perpendicular to the field. In the absence of easy-plane anisotropy, the rotational symmetry about the z axis will produce domains that cancel the net M_y spin. The solutions for both the NC-3i and NC-3ii states are checked by assuring that every spin $\mathbf{S}_i$ in the 3-SL unit cell is locally in equilibrium. These spin states were first predicted by Miyashita [24] for a triangular-lattice AF with nearest-neighbor interactions only ($J_2 = J_3 = 0$).

When $D_\perp = 0$, another trial spin state may be introduced for the conical spin-flop (SF) phase: $S_x(\mathbf{R}) = S\sqrt{1-M^2}\cos(Qx)$, $S_y(\mathbf{R}) = S\sqrt{1-M^2}\sin(Qx)$, and $S_z(\mathbf{R}) = SM$. Because the anisotropy D acts along the z axis, the SF state does not contain anharmonic components in the xy plane and the trial SF state contains only two variational parameters, Q and M. The SF phase played an important role in the phase diagram of $CuFeO_2$ [25]. Within region 4ii, the SF state with lowest energy has $Q = 4\pi/3$. In zero field, this state is the 120° phase with spins in the xy plane. If $D > 0$, the SF state always has a higher energy than the NC-3i and NC-3ii states due to their extra anisotropy energy. The degeneracy between the SF and NC-3 states when $D = 0$ would be broken in favor of the NC-3 states by easy-plane anisotropy $D_\perp < 0$.

Figure 2 presents the resulting magnetic phase diagrams of a triangular-lattice AF in subregion 4ii for points corresponding to the dot or diamond in figure 1(g). Although the CL-5i appeared in the predicted phase diagram of $CuFeO_2$ [25] and was observed [11] at fields above 13.5 T, it is absent from the predicted phase diagram of $CuCrO_2$ when $J_2 > -|J_1|/3$. It does, however, appear in the phase diagram when $J_2 < -|J_1|/3$ as the narrow wedge between the CL-4 and CL-3 phases shown in figure 2(b). Besides the appearance of the CL-5i phase, the phase diagrams within subregion 4ii for $J_2 > -|J_1|/3$ and $J_2 < -|J_1|/3$ are qualitatively similar.

In figure 3(a), the normalized spin M_z is plotted versus field for several values of $D/|J_1|$ using the same exchange parameters as in figure 2(a). While the NC-3i → CL-3 transition is second order, the CL-3 → NC-3ii transition is first order at a sufficiently large field. On the other hand, the NC-3ii → CL-1 transition is second order with a gradual saturation of M_z as the spins tilt toward the z axis with increasing field.

The absolute value of the spontaneous transverse spin M_y in the NC-3ii phase is plotted versus field in the inset to figure 3(b). Like M_z, $|M_y|$ also exhibits a jump at the first-order CL-3 → NC-3ii transition. However, $|M_y|$ smoothly vanishes at the second-order NC-3ii → CL-1 transition. A phase with a spontaneous transverse moment does not appear in the predicted phase diagram of $CuFeO_2$ [25].

As expected, the deviation of the NC-3 state from a perfect spiral increases with the anisotropy D. For zero field, ϕ increases from 120° to 129.5° and M_z increases from 0 to 0.091 as $D/|J_1|$ increases from 0 to 0.68, which is the NC-3i → CL-4 phase boundary.

Figure 3(b) plots the amplitude of the chirality $\mathbf{C} = \langle\mathbf{S}(\mathbf{R}) \times \mathbf{S}(\mathbf{R}+\mathbf{x}/2)\rangle/S^2$ versus field. As expected, the NC-3ii state is not chiral. For the NC-3i state, $\mathbf{C}$ lies along the x axis. The chirality decreases with the anisotropy and smoothly vanishes with increasing field at the second-order NC-3i → CL-3 phase transition.

[1] Because the conditions for global and local stability are different, the boundary between the CL-4 subregions is slightly shifted from that given in [20]. See [21].

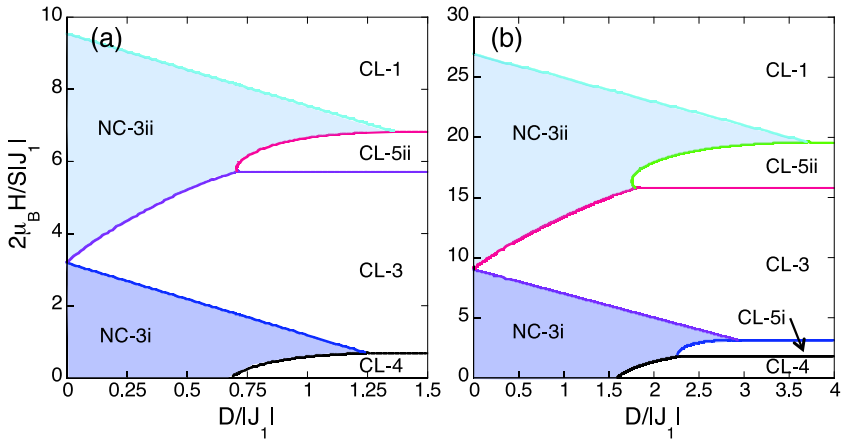

Figure 2. Magnetic phase diagrams as a function of external field and anisotropy for $\{J_2/|J_1|, J_3/|J_1|\}$ given by (a) $\{-0.11, -0.06\}$ or (b) $\{-0.38, -2\}$, corresponding to the dot or diamond in figure 1(g). NC phases are shaded.

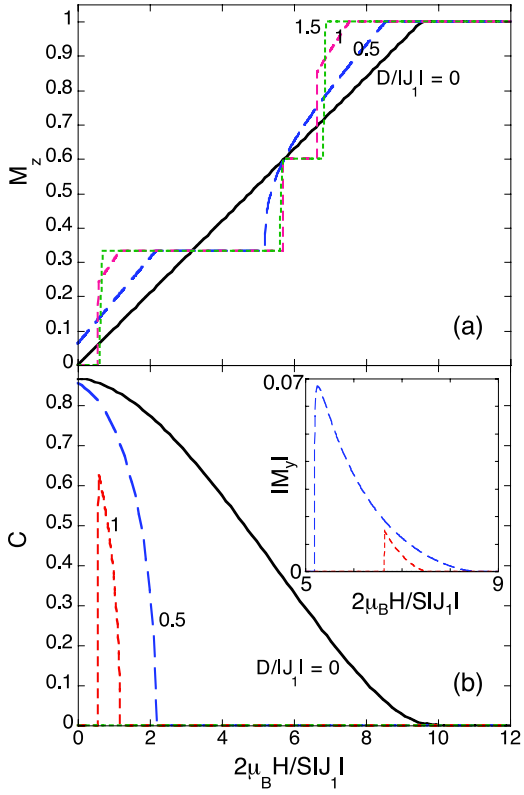

Figure 3. (a) The net normalized spin M_z and (b) the chirality C as a function of field for $D/|J_1| = 0$, 0.5, 1. and 1.5. Inset in (b) is the spontaneous transverse spin $|M_y|$ for the non-chiral NC-3ii phase. Exchange parameters as in figure 2(a), corresponding to the dot in figure 1(g).

The phase diagrams obtained in this paper qualitatively agree with Miyashita [24], who studied a triangular-lattice AF with only nearest-neighbor exchange ($J_2 = J_3 = 0$). When $D = 0$, the NC-3i and NC-3ii phases appear on either side of the field $2\mu_B H_c = 3|J_1|S$ and the CL-3 phase intercedes between the two NC phases when $D > 0$. The main difference between the phase diagrams with and without exchanges J_2 and J_3 is that the CL-4 and CL-5 phases are absent in the phase diagram obtained by Miyashita. Also for the triangular-lattice AF with nearest-neighbor exchange, Chubukov and Golosov [26] found that quantum spin fluctuations have similar effects as the anisotropy: opening a magnetization plateau for the CL-3 phase with $M_z = 1/3$ and stabilizing the coplanar phases over the SF phase when $D = 0$.

Based on the value $J_1 = -2.3$ meV [13] and the results of figure 2(a), we estimate that the critical field H_c for the NC-3i $\rightarrow$ CL-3 transition is slightly smaller than 95 T. This estimate agrees remarkably well with the low-temperature susceptibility of $\chi = 5.9 \times 10^{-3}$ emu mol^{-1} measured for $CuCrO_2$ [6], which yields a normalized spin $M = 1/3$ or a magnetization of 1 μ_B/Cr ion at a field of 94.7 T. Recent pulsed measurements [6] found no signature of a phase transition up to 53 T.

By contrast, the multiferroic phase of $CuFeO_2$ is sandwiched between critical fields $H_{c1} \sim 0.5S|J_1|/\mu_B$ and $H_{c2} \sim S|J_1|/\mu_B$ [25]. Using $S = 5/2$ and $J_1 \approx -0.23$ meV [22] yields critical fields of 5 and 10 T, slightly smaller than the observed critical fields of 7 and 13.5 T [11]. Hence, the upper critical field for the multiferroic phase in $CuCrO_2$ is much larger than the critical fields in $CuFeO_2$ mainly because of its much larger $|J_1|$.

Despite the rather high upper critical field for the multiferroic phase of $CuCrO_2$, it may be possible to observe the effects of a magnetic field in other ways. If the multiferroic properties of $CuCrO_2$ are directly related to the chirality of the NC state, the ferroelectric coupling of $CuCrO_2$ should decrease with field. For example, figure 3(a) implies that the chirality of the NC-3i phase decreases by about 13% in a 50 T field. The direct effect of a magnetic field on the NC-3i state may also be possible to measure. For $D = 0$, ϕ increases from 120° to 131.1° as H increases from 0 to 30 T. It may also be possible to lower the upper critical field with oxygen nonstoichiometry, which is expected to enhance the anisotropy.

To conclude, we have used a simple two-dimensional model to qualitatively predict the magnetic phase diagram of multiferroic $CuCrO_2$. Although significant quantum

fluctuations cannot be ruled out for a spin-3/2 material, the excellent results obtained from the $1/S$ expansion used to model the inelastic spectrum [14] suggest that a classical model is a good starting point to describe the behavior of $CuCrO_2$. So we are hopeful that new high-field sources may soon be able to access the predicted 3-SL CL phase at about 95 T.

Acknowledgments

I would like to acknowledge helpful conversations with Sasha Chernyshev, Georg Ehlers, Matthias Frontzek, Jason Haraldsen, and Satoshi Okamoto. Research sponsored by the US Department of Energy, Office of Basic Energy Sciences, Materials Sciences and Engineering Division.

References

[1] Khomskii D I 2006 *J. Magn. Magn. Mater.* **306** 1
Cheong S-W and Mostovoy M 2007 *Nature Mater.* **6** 13
[2] Katsura H, Nagaosa N and Balatsky A V 2005 *Phys. Rev. Lett.* **95** 057205
Mostovoy M 2006 *Phys. Rev. Lett.* **96** 067601
[3] Mitsuda S, Yoshizawa H, Yaguchi N and Mekata M 1991 *J. Phys. Soc. Japan* **60** 1885
[4] Nakajima T, Mitsuda S, Kanetsuki S, Prokes K, Podlesnyak A, Kimura H and Noda Y 2007 *J. Phys. Soc. Japan* **76** 043709
Nakajima T, Mitsuda S, Kanetsuki S, Tanaka K, Fujii K, Terada N, Soda M, Matsuura M and Hirota K 2008 *Phys. Rev.* B **77** 052401
[5] Seki S, Onose Y and Tokura Y 2008 *Phys. Rev. Lett.* **101** 067204
[6] Kimura K, Nakamura H, Ohgushi K and Kimura T 2008 *Phys. Rev.* B **78** 140401(R)
Kimura K, Nakamura H, Kimura S, Hagiwara M and Kimura T 2009 *Phys. Rev. Lett.* **103** 107201
Soda M, Kimura K, Kimura T and Hirota K 2010 *Phys. Rev.* B **81** 100406
[7] Jia C, Onoda S, Nagaosa N and Han J H 2006 *Phys. Rev.* B **74** 224444
[8] Arima T 2007 *J. Phys. Soc. Japan* **76** 073702
[9] Kadowaki H, Kikuchi H and Ajiro Y 1990 *J. Phys.: Condens. Matter* **2** 4485
Kadowaki H, Takei H and Motoya K 1995 *J. Phys.: Condens. Matter* **7** 6869
[10] Seki S, Yamasaki Y, Shiomi Y, Iguchi S, Onose Y and Tokura Y 2007 *Phys. Rev.* B **75** 100403(R)
Kanetsuki S, Mitsuda S, Nakajima T, Anazawa D, Katori H A and Prokes K 2007 *J. Phys.: Condens. Matter* **19** 145244
[11] Mitsuda S, Mase M, Prokes K, Kitizawa H and Katori H A 2000 *J. Phys. Soc. Japan* **69** 3513
[12] Kimura T, Lashley J C and Ramirez A P 2006 *Phys. Rev.* B **73** 220401(R)
[13] Poienar M, Damay F, Martin C, Robert J and Petit S 2010 *Phys. Rev.* B **81** 104411
[14] Frontzek M, Haraldsen J T, Podlesnyak A, Matsuda M, Christianson A, Fishman R S, Qiu Y, Copley J, Barilo S, Shiryaev S V and Ehlers G 2011 *Phys. Rev.* B submitted
[15] Terada N, Mitsuda S, Oshumi H and Tajima K 2006 *J. Phys. Soc. Japan* **75** 23602
Ye F, Ren Y, Huang Q, Fernandez-Baca J A, Dai P, Lynn J W and Kimura T 2006 *Phys. Rev.* B **73** 220404
[16] Kimura K, Otani T, Nakamura H, Wakabayashi Y and Kimura T 2009 *J Phys. Soc. Japan* **78** 113710
[17] Haraldsen J T, Ye F, Fishman R S, Fernandez-Baca J A, Yamaguchi Y, Kimura K and Kimura T 2010 *Phys. Rev.* B **82** 020404
Haraldsen J T and Fishman R S 2010 *Phys. Rev.* B **82** 144441
[18] Hasegawa M, Batrashevich M I, Zhao T R, Takei H and Goto T 2001 *Phys. Rev.* B **63** 184437
[19] Takagi T and Mekata M 1995 *J. Phys. Soc. Japan* **64** 4609
[20] Swanson M, Haraldsen J T and Fishman R S 2009 *Phys. Rev.* B **79** 184413
Haraldsen J T, Swanson M, Alvarez G and Fishman R S 2009 *Phys. Rev. Lett.* **102** 237204
[21] Fishman R S and Haraldsen J T 2011 *J. Appl. Phys.* **109** 07E117
[22] Ye F, Fernandez-Baca J A, Fishman R S, Ren Y, Kang H J, Qiu Y and Kimura T 2007 *Phys. Rev. Lett.* **99** 157201
Fishman R S, Ye F, Fernandez-Baca J A, Haraldsen J T and Kimura T 2008 *Phys. Rev.* B **78** 140407(R)
[23] Fishman R S and Okamoto S 2010 *Phys. Rev.* B **81** 020402(R)
[24] Miyashita S 1986 *J. Phys. Soc. Japan* **55** 3605
[25] Fishman R S 2011 *Phys. Rev. Lett.* **106** 037206
[26] Chubukov A V and Golosov D I 1991 *J. Phys.: Condens. Matter* **3** 69